Center for Turbulence Research
Proceedings of the Summer Program 2018

Large-scale space definition for the DG-VMS method based on energy transfer analyses

By F. Naddei†, M. de la Llave Plata†, E. Lamballais‡, V. Couaillier†, M. Massot¶ AND M. Ihme

A-priori analyses to study the effect of the large-scale space definition in the variational multiscale simulation (VMS) approach to LES are carried out in the context of a modal discontinuous Galerkin (DG) method. A numerically consistent framework is introduced to derive the expression of the ideal subgrid-scale (SGS) energy transfer, which takes into account the different terms involved in the DG discretization. Based on the insight gained from this study, a locally adaptive modeling strategy able to adjust the definition of the large-scale space to the local resolution requirements of the flow is proposed.

1. Introduction

The use of DG methods in the context of scale-resolving simulations has seen a rapid increase in recent years, particularly due to their excellent parallel scalability and their ability to achieve high-order accuracy on general meshes (Cockburn & Shu 2001).

The variational framework on which these methods rely also allows for the local separation of scales using the polynomial basis functions. This feature is most useful in the development of multiscale LES techniques. In particular, the VMS approach introduced in Hughes *et al.* (2000) offers an interesting alternative to traditional LES approaches. The fundamental assumption of this approach is that the large-scale dynamics are virtually free from SGS dissipation. However, the validity of such an assumption strongly depends on the considered problem (e.g., Reynolds number and grid resolution) as well as on the properties of the scale-separation operator (Sagaut & Levasseur 2005).

In most works found in the literature on VMS, the scale separation is defined either heuristically or, alternatively, *a-posteriori* by performing simulations of a given configuration based on different definitions of the large-scale space. These approaches present serious limitations, especially when dealing with inhomogeneous or (statistically) unsteady turbulence simulations that require the adaptation of the scale-partition parameter in space and/or time.

The main goal of this research is therefore to extend the current understanding of the VMS approach to the context of a modal DG method and to develop a methodology enabling a systematic use of the DG-VMS technique. To this end, the spectral analyses performed by Sagaut & Levasseur (2005) and Hughes *et al.* (2004) using sharp cut-off (orthogonal) filters are extended to the DG framework, thus relying on variational projection (non-orthogonal filtering in Fourier space). This is achieved by performing *a-priori* analyses based on the projection of reference DNS data of the Taylor-Green

† Department of Aerodynamics, Aeroelasticity and Acoustics, ONERA, France
‡ Institute PPRIME, Université de Poitiers, France
¶ Centre for Applied Mathematics, École Polytechnique, France

vortex (TGV) configuration at $Re = 5,000$ and $20,000$ (Dairay *et al.* 2017) onto different LES *hp*-discretizations (h denoting the characteristic mesh size and p the degree of the polynomial approximation). The focus is on studying the spectral properties of the SGS energy transfer provided by the DG-VMS approach. Based on the outcome from this study, a local (in space and time) model-adaptive strategy is proposed. The accuracy of this new approach is illustrated *a-posteriori* on the TGV flow configuration at $Re = 5,000$.

2. A-priori analysis

A-priori testing can provide valuable information about the accuracy of LES modeling approaches. The central question with this type of analysis is the definition of an appropriate ideal LES solution, which in the general case is not straightforward. It is, however, essential to answer this question, as the way in which this ideal solution is defined will have a direct impact on the way the ideal SGS quantities are computed. The classical approach relies on defining the ideal LES solution as that obtained from the spatially filtered Navier-Stokes (N-S) equations. This approach entirely ignores the details of the discretization employed and the fact that the LES solution so defined might not be an admissible solution of the considered discrete problem. A second approach has been proposed by Pope (2001), in which the LES solution is conceived as the projection of the DNS solution onto a set of local basis functions. This has been shown by Vreman (2004) to actually correspond to the application of a non-uniform filter kernel. This methodology provides a definition of the ideal resolved field which is consistent with the employed numerical discretization. However, this projection can introduce significant aliasing errors at wavenumbers close to the grid cutoff, producing unphysical reference data. This is a direct consequence of the approximation properties of polynomial basis functions [see Gottlieb & Orszag (1977)].

In this work we propose to employ an alternative approach in which the ideal DG-LES solution is defined as the result of the application of two successive filtering operations. A first convolution filter is applied to the DNS data which filters out frequencies beyond the LES grid cutoff. Next, a L^2-projection of this filtered field is performed on the *hp*-discretization space (DG filter). This procedure reduces considerably the aliasing errors introduced by Pope's approach, while allowing the inclusion in the analysis of the effect of the *hp*-discretization associated with the adopted numerical method.

The following section provides a formal framework for the definition of the ideal DG-LES solution as described above and the expression of the corresponding ideal SGS energy transfer.

2.1. *The DG-LES framework and the ideal energy transfer*

The N-S equations for an incompressible flow read

$$\frac{\partial \mathbf{u}}{\partial t} + \boldsymbol{\nabla} \cdot \mathcal{F}_c(\mathbf{u}, q) + \boldsymbol{\nabla} \cdot \mathcal{F}_d(\mathbf{u}, \boldsymbol{\nabla}\mathbf{u}) = 0 \ , \qquad \forall \mathbf{x} \in \Omega, t \geq 0 \ , \tag{2.1}$$

$$\boldsymbol{\nabla} \cdot \mathbf{u} = 0 \ , \tag{2.2}$$

where $\mathbf{u}$ is the velocity field, q is the pressure, and $\mathcal{F}_c$ and $\mathcal{F}_d$ are the convective and diffusive fluxes, respectively. Let us denote by $\overline{(\cdot)}$ a spatial convolution filtering operation that is defined for any function f as, $\overline{f}(x) := \int_\Omega G(x-\xi) f(\xi) \mathrm{d}\xi$. We define Ω_K to be a shape regular partition of Ω into N non-overlapping, non-empty elements. We further

define the broken Sobolev space $S_h^p := \{\phi \in L^2(\Omega_K) : \phi|_K \in \mathcal{P}^p(K), \forall K \in \Omega_K\}$ to be the space of piecewise polynomials of order at most p. We indicate as $\{\phi_K^1 \dots \phi_K^{N_p}\} \in \mathcal{P}^p(K)$ a hierarchical orthonormal basis for $\mathcal{P}^p(K)$ with $\phi_K^i(\mathbf{x}) = 0, \forall \mathbf{x} \in K', K' \neq K$. Then we indicate $f_h := \mathbb{P}_{S_h^p}(f)$ as the projection of any function f on the *hp*-discretization defined by the space S_h^p.

Following the approach described in the previous section, we define the ideal DG-LES solution as $\overline{\mathbf{u}}_h := \mathbb{P}_{S_h^p}(\overline{\mathbf{u}})$, which is the result of the successive application of a convolution filter and the DG filter defined by the space S_h^p to the velocity field $\mathbf{u}$. In the *a-priori* analysis presented in the next section, we consider this convolution filter to be a sharp cut-off filter in Fourier space, with cut-off wavenumber corresponding to $k_c = (p+1)/(2h)$.

Starting from Eq. (2.1), the evolution equations for the ideal DG-LES solution therefore read

$$\begin{aligned}\frac{\partial}{\partial t}\int_{\Omega_K} \overline{\mathbf{u}}_h \phi \,\mathrm{d}\mathbf{x} + \sum_K \Bigg[\int_{\partial K} \overline{\mathcal{F}}_d(\mathbf{u}, \boldsymbol{\nabla}\mathbf{u}) \cdot \mathbf{n}^+ \phi^+ \,\mathrm{d}\sigma - \int_K \overline{\mathcal{F}}_d(\mathbf{u}, \boldsymbol{\nabla}\mathbf{u}) \cdot \boldsymbol{\nabla}\phi \,\mathrm{d}\mathbf{x} \\ + \int_{\partial K} \overline{\mathcal{F}}_c(\mathbf{u}, q) \cdot \mathbf{n}^+ \phi^+ \,\mathrm{d}\sigma - \int_K \overline{\mathcal{F}}_c(\mathbf{u}, q) \cdot \boldsymbol{\nabla}\phi \,\mathrm{d}\mathbf{x} \Bigg] = 0 \,, \quad \forall \phi \in S_h^p \,,\end{aligned} \tag{2.3}$$

where we have used the fact that the convolution filter commutes with the spatial derivatives and the definition of the L^2-projection, i.e., $\int_{\Omega_K} (\overline{\mathbf{u}} - \overline{\mathbf{u}}_h)\phi = 0, \forall \phi \in S_h^p$.

The DG-LES equations can now be defined by rewriting Eq. (2.3) as

$$\begin{aligned}\frac{\partial}{\partial t}\int_{\Omega_K} \overline{\mathbf{u}}_h \phi \,\mathrm{d}\mathbf{x} + \sum_K \left[\int_{\partial K} \mathbf{h}_c(\overline{\mathbf{u}}_h^+, \overline{q}_h^+, \overline{\mathbf{u}}_h^-, \overline{q}_h^-, \mathbf{n}^+)\phi^+ \,\mathrm{d}\sigma - \int_K \mathcal{F}_c(\overline{\mathbf{u}}_h, \overline{q}_h) \cdot \boldsymbol{\nabla}\phi \,\mathrm{d}\mathbf{x} \right] + \\ \sum_K \left[\int_{\partial K} \mathbf{h}_d(\overline{\mathbf{u}}_h^+, \overline{\mathbf{u}}_h^-, \mathbf{n}^+)\phi^+ \,\mathrm{d}\sigma - \int_K \mathcal{F}_d(\overline{\mathbf{u}}_h) \cdot \boldsymbol{\nabla}\phi \,\mathrm{d}\mathbf{x} \right] + \mathcal{R}(\mathbf{u}, \overline{\mathbf{u}}_h, \phi) = 0 \,, \quad \forall \phi \in S_h^p \,,\end{aligned} \tag{2.4}$$

where $\mathbf{h}_c$ and $\mathbf{h}_d$ are the convective and diffusive numerical fluxes, respectively. In Eq. (2.4), $\mathcal{R}(\mathbf{u}, \overline{\mathbf{u}}_h, \phi)$ is the subgrid residual representing the effect of the unresolved scales $\mathbf{u} - \overline{\mathbf{u}}_h$ on the resolved field, which can be obtained by comparing Eq. (2.3) and Eq. (2.4). In this work, we assume that the SGS term is dominated by convective effects. The contribution of the viscous and pressure terms is thereby neglected. This leads to the following form for the subgrid residual,

$$\begin{aligned}\mathcal{R}(\mathbf{u}, \overline{\mathbf{u}}_h, \phi) = \sum_K \Bigg[\int_K \left(\mathcal{F}_c(\overline{\mathbf{u}}_h) - \overline{\mathcal{F}}_c(\mathbf{u}) \right) \cdot \boldsymbol{\nabla}\phi \,\mathrm{d}\mathbf{x} \\ - \int_{\partial K} \left(\mathbf{h}_c(\overline{\mathbf{u}}_h^+, \overline{\mathbf{u}}_h^-, \mathbf{n}^+) - \overline{\mathcal{F}}_c(\mathbf{u}) \cdot \mathbf{n}^+ \right) \phi^+ \,\mathrm{d}\sigma \Bigg] \,.\end{aligned} \tag{2.5}$$

The ideal energy transfer from the resolved modes of wavenumber k to all unresolved scales can now be obtained from the subgrid residual as

$$T_{sgs}(k) = \sum_{\|\mathbf{k}\|=k} \widehat{\overline{\mathbf{u}}_h}(\mathbf{k}) \cdot \widehat{\mathrm{R}}(\mathbf{k}) \,, \quad \text{with} \quad \mathrm{R}(\mathbf{x}) = \sum_K \sum_i \mathcal{R}(\mathbf{u}, \overline{\mathbf{u}}_h, \phi_K^i)\phi_K^i(\mathbf{x}) \,, \tag{2.6}$$

where $\widehat{(\cdot)}$ denotes the Fourier transform and R represents the subgrid residual in the physical domain.

Note that the use of the DG-projection filter introduces discontinuities in the filtered

velocity field that need to be taken into account and require the definition of the numerical flux $\mathbf{h}_c$ that appears in the surface integral in Eq. (2.5). The subgrid stress thus depends in general on both the definition of the filter and the choice of this numerical flux. In this work we employ a symmetrical numerical flux $\mathbf{h}_c = 1/2(\mathcal{F}_c(\overline{\mathbf{u}}_h^+) + \mathcal{F}_c(\overline{\mathbf{u}}_h^-)) \cdot \mathbf{n}^+$, thus allowing the evaluation of $\mathrm{R}(\mathbf{x})$ in the absence of numerical dissipation. This methodology provides a rigorous framework for the derivation of the ideal energy transfer that is consistent with the employed discretization.

2.2. *The DG-VMS approach and the modeled energy transfer*

Starting from Eq. (2.4), the effect of the subgrid scales can be approximated by a model term that depends only on the resolved field $\mathcal{R}(\mathbf{u}, \overline{\mathbf{u}}_h, \phi) \approx \mathcal{L}_m(\overline{\mathbf{u}}_h, \phi)$. To this end, we can use for example an eddy-viscosity approach, such as the Smagorinsky model.

In VMS we assume that the effect of the unresolved scales on the largest resolved scales is negligible and thus the effect of the SGS model is confined to a range of small resolved scales. This is obtained in the DG-VMS framework by splitting the polynomial space S_h^p into a low-order component $\mathcal{V}^l \equiv S_h^{p_L} \subseteq S_h^p$ associated with the large scales and a high-order component $\mathcal{V}^s \equiv S_h^p \setminus \mathcal{V}^l$ representing the small scales, where p_L is called the scale-partition parameter. In this work, the SGS term is computed from the full resolved field, as done by Chapelier *et al.* (2016), and the effect of the SGS model is removed from all scales belonging to $\mathcal{V}^l$ by enforcing $\mathcal{L}_m(\overline{\mathbf{u}}_h, \phi) = 0, \forall \phi \in \mathcal{V}^l$.

The modeled energy transfer in DG-VMS can then be written as

$$T_m(k) = \sum_{\|\mathbf{k}\|=k} \widehat{\overline{\mathbf{u}}_h}(\mathbf{k}) \cdot \widehat{\mathrm{L}}_m(\mathbf{k}) \quad \text{with} \quad \mathrm{L}_m(\mathbf{x}) = \sum_K \sum_i \mathcal{L}_m(\overline{\mathbf{u}}_h, \phi_K^i)\phi_K^i(\mathbf{x}). \tag{2.7}$$

2.3. *Results from a-priori testing*

The methodology laid out in the previous section is applied to two DNS data sets of the TGV configuration at $Re = 5,000$ and $20,000$, with spatial resolution corresponding to 1280^3 and 3456^3 degrees of freedom (dofs), respectively. A snapshot of each of these data sets at $t = 14$ (non-dimensional time units) is selected for analysis.

The ideal energy transfer, defined by Eq. (2.6), is compared to that provided by the DG-VMS based on the Smagorinsky model for different *hp*-discretizations and values of the scale-partition parameter p_L. For each configuration, three *hp*-discretizations are considered, corresponding respectively to $1/16^3$, $1/8^3$, and $1/4^3$ of the DNS resolution for $Re = 5,000$, and $1/36^3$, $1/18^3$, and $1/9^3$ of the DNS resolution for $Re = 20,000$. Figure 1 presents the energy spectra of the DNS velocity fields. The cut-off wavenumbers corresponding to the selected resolutions are also shown in this figure; they are equal to half the number of dofs of the considered *hp*-discretizations, namely $k_c = (p+1)/(2h)$.

For the configuration at $Re = 5,000$, Figure 2(a) shows the ideal and modeled energy transfer obtained for the coarsest resolution considered, for which the associated cut-off frequency is located at the end of the inertial range [see Figure 1(a)]. As seen from this plot, for this particular resolution the interaction between the large and the unresolved scales is non-negligible and the dissipation provided by the Smagorinsky model is in good agreement with the ideal energy transfer. Note that the Smagorinsky model is actually equivalent to the DG-VMS approach in which the model is applied to all resolved scales.

For higher resolutions (Figure 2(b) and (c)) the ideal energy transfer is negligible at low wavenumbers and presents the expected cusp-like behavior toward the upper end of the spectrum. In this case, the Smagorinsky model provides an excessive amount of dissipation, whereas the DG-VMS approach appears in fairly good agreement with the

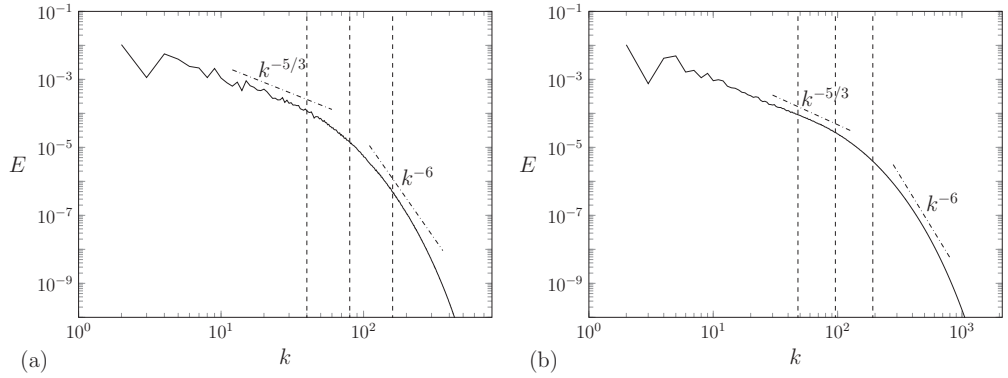

FIGURE 1. Energy spectra for the TGV at (a) $Re = 5,000$ and (b) $Re = 20,000$ at $t = 14$. Dashed lines correspond to the resolutions considered in the evaluation of the energy transfer.

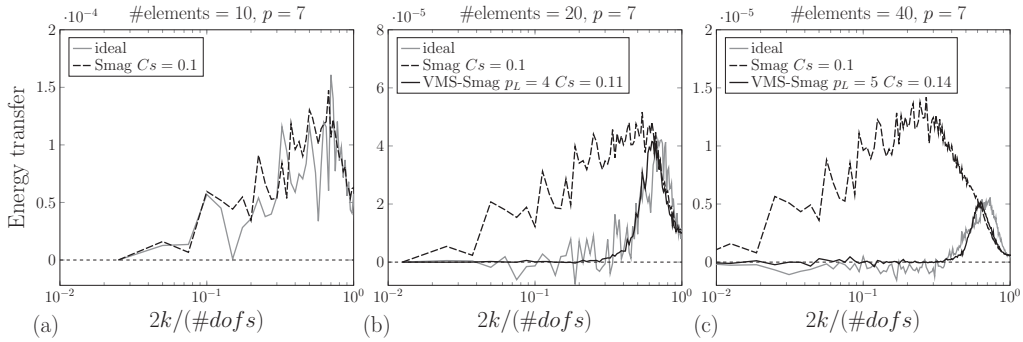

FIGURE 2. TGV at $Re = 5,000$: spectral energy transfer for the ideal subgrid stress, the standard Smagorinsky model and the DG-VMS model for three DG-LES resolutions.

reference values for an optimal choice of the model parameters C_s and p_L. The values of these parameters are reported in the corresponding legends on the top left corner of each of these plots. As expected, when the resolution is increased, the optimal value of p_L also increases, moving from $p_L = 4$ to $p_L = 5$. Another interesting feature of the modeled energy transfer is the smooth transition it displays between its plateau values and its value at the peak, which indicates that the DG-VMS scale-separation operator is equivalent to a non-orthogonal filter in Fourier space [see Sagaut & Levasseur (2005)]. Finally, it is worth noting that, for these two higher resolutions, the peak of the modeled energy transfer is slightly shifted to the left with respect to the ideal one. This would suggest that a minimum amount of numerical dissipation is still necessary to cover the full ideal dissipation spectrum. This is in agreement with our observations in *a-posteriori* DG-VMS tests, for which a minimum amount of numerical dissipation is always necessary to stabilize the simulation.

These results suggest that an adaptive DG-VMS approach able to adjust the model parameters both in space and time could considerably improve the quality of the simulation with respect to the standard approach. Note that in an actual simulation the resolution requirements might change across space and over time, which points to the necessity of developing a space-time adaptive method able to dynamically adjust and redistribute the amount of SGS dissipation in modal space.

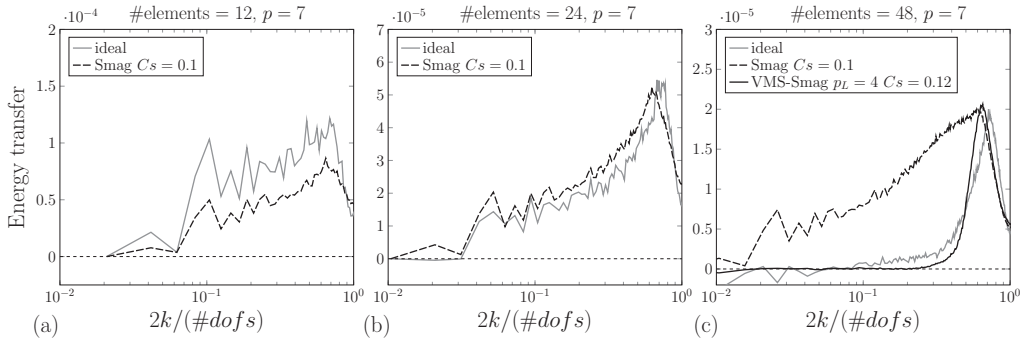

FIGURE 3. TGV at $Re = 20,000$: spectral energy transfer for the ideal subgrid stress, the standard Smagorinsky model and the DG-VMS model for three DG-LES resolutions.

For the higher Reynolds number case at $Re = 20,000$, the results shown in Figure 3 corroborate the conclusions drawn from the lower Reynolds number configuration. One notable difference can be observed however for the intermediate resolution, which corresponds to a cut-off frequency located at the beginning of the dissipation range [see Figure 1(b)]. This is the coexistence of both a non-negligible interaction between the large and the unresolved scales and a peak of energy transfer at a frequency close to the cutoff. This can be interpreted as the presence of a non-zero plateau of the effective eddy viscosity, already observed by Lamballais *et al.* (2017) for this same configuration and in theoretical analyses considering an infinite inertial range. It appears that in this situation the appropriate combination of the standard Smagorinsky and VMS approaches could lead to improved results.

3. A new adaptive DG-VMS algorithm

Based on the insights gained from the previous section, we propose here an adaptive algorithm able to dynamically adapt the value of the scale-partition parameter p_L in the DG-VMS approach. To this end, we start by defining the large-scale space as $\mathcal{V}^l = \{\phi \in S_h^p, \phi|_K \in P^{p_L^K}(K) \text{ if } p_L^K \geq 0, \phi|_K = 0 \text{ if } p_L^K = -1\}$ where $-1 \leq p_L^K \leq p$ is the local scale-partition parameter. The value p_L^K is selected based on the decay rate of the momentum energy in modal space, which provides a measure of the local smoothness of the solution in each element. The modal energy is defined as

$$E_K^{\{j\}} := \int_K (\rho\mathbf{u})^{\{j\}} \cdot (\rho\mathbf{u})^{\{j\}} \mathrm{d}\mathbf{x} \,, \tag{3.1}$$

where $(\rho\mathbf{u})^{\{j\}}$ for $0 \leq j \leq p$ is the projection of the resolved momentum density on the space $S_h^j \setminus S_h^{j-1}$. It is assumed that, for a sufficiently resolved field, the modal energy follows a power law, namely, $E_K^{\{j\}} \propto (j+1)^{-\sigma_K}$, where the decay rate exponent σ_K is obtained by means of a least-square method. The idea of using the spectral slope to develop dynamic SGS models was originally proposed by Lamballais *et al.* (1998) in the context of a high-order finite-difference scheme. A similar smoothness measure has been employed recently by Chapelier & Lodato (2016) to develop a dynamic eddy-viscosity model based on a high-order spectral difference method.

The relevance of this approach in the context of VMS is demonstrated by the results obtained in our *a-priori* analysis. Indeed, as reported in the previous section, if the filter

cut-off wavenumber is located in the inertial range, $E(k) \propto k^{-\frac{5}{3}}$, the Smagorinsky model can provide the ideal distribution of energy transfer over all resolved scales. In contrast, if the cut-off wavenumber is located in the dissipation range, $E(k) \propto k^{-\alpha}$, $\alpha > 5/3$, the DG-VMS approach with $p_L \geq 0$ can more accurately approximate the physical energy transfer from resolved to unresolved scales. Thus, the slope of the spectrum α can provide an indication of the range of applicability of the VMS approach. It has been verified *a-priori* that the exponent σ_K provides very similar information, with the additional advantage that it can be computed locally within an element and with limited computational overhead, as the modal coefficients are readily available.

The value σ_K is therefore computed over the course of the simulation for each element K, and p_L^K is locally set as

$$p_L^K(\sigma_K) = \begin{cases} \text{round}\left[(p+1)\left(\frac{\sigma_K - \sigma_{th}}{\beta + \sigma_K - \sigma_{th}}\right) - 1\right], & \text{if } \sigma_K \geq \sigma_{th}\ , \\ -1 \qquad\qquad\qquad\qquad\qquad\quad , & \text{if } \sigma_K < \sigma_{th}\ . \end{cases} \tag{3.2}$$

In Eq. (3.2), the value of the threshold σ_{th} represents the level of smoothness under which the SGS dissipation is applied to all scales represented within the element. The additional parameter β is related to the rate of change of p_L^K. This relation therefore allows us to recover the Smagorinsky model for highly under-resolved regions when $\sigma_K \leq \sigma_{th}$ and yields high values of p_L^K in sufficiently resolved zones. In the limit case $\sigma_K \to \infty$, we have that $p_L^K \to p$, and no SGS dissipation is applied, which corresponds to locally using a no-model approach, also called implicit LES (ILES).

The value of the threshold σ_{th} has been estimated in *a-priori* tests carried out for $Re = 5,000$ on the coarsest resolution considered, for which the Smagorinsky model matches the ideal energy transfer [see Figure 2]. A value of σ_{th} between 1.8 and 2 has been obtained by considering the solution at different times between $t = 14$ and $t = 20$ (fully developed turbulence). The sensitivity of the solution to this parameter is analyzed in the *a-posteriori* tests described below.

3.1. *Results from a-posteriori testing*

The proposed algorithm is evaluated by performing simulations of the TGV configuration at $Re = 5,000$ and Mach number $M = 0.1$, using the DG solver *Aghora* [see Chapelier *et al.* (2016)]. The *hp*-discretization considered consists of 12^3 elements and a polynomial degree $p = 7$. Unless stated otherwise, the discretization of the convective fluxes is carried out using a low-dissipative version of the Roe scheme for which the upwind component has been scaled by a parameter $\alpha_{Roe} = 0.1$. The discretization of the viscous and SGS model terms is performed based on the BR2 scheme. An explicit third-order strong stability-preserving Runge-Kutta scheme with time step $\Delta t = 5 \cdot 10^{-4}$ is used for time integration. For de-aliasing purposes, the evaluation of the integrals employs $(3p+1)/2$ quadrature points per space direction.

The adaptive DG-VMS approach based on a value of $\sigma_{th} = 1.8$ and $\beta = 0.7$ is compared to the standard DG-VMS with $p_L = 5$, which corresponds to a fraction of large scales equal to 75%, as recommended in the literature on VMS. These simulations are compared to reference data obtained by filtering the DNS data following the procedure described in section 2.3. We also report the results corresponding to an ILES for which the only source of dissipation is that introduced by the upwind component of the Roe scheme ($\alpha_{Roe} = 1$). For all model-based simulations, the Smagorinsky constant is set to $C_s = 0.1$.

Figure 4 illustrates the evolution over time of the resolved kinetic energy $\mathcal{K}$ and

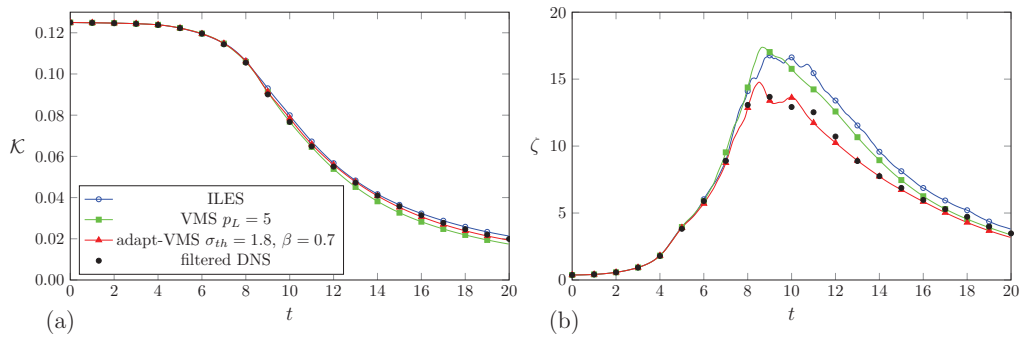

FIGURE 4. TGV at $Re = 5,000$: evolution of the (a) resolved kinetic energy and (b) enstrophy.

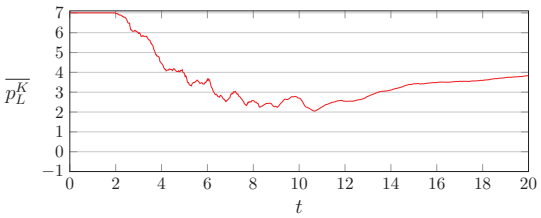

FIGURE 5. TGV at $Re = 5,000$: evolution of the average scale-partition parameter for $\sigma_{th} = 0.18$ and $\beta = 0.7$.

enstrophy ζ, given respectively by

$$\mathcal{K} = \frac{1}{2V}\int_\Omega \rho \mathbf{u}\cdot\mathbf{u}\mathrm{d}\mathbf{x}\ , \qquad \zeta = \frac{1}{V}\int_\Omega (\boldsymbol{\nabla}\times\mathbf{u})\cdot(\boldsymbol{\nabla}\times\mathbf{u})\mathrm{d}\mathbf{x}\ . \tag{3.3}$$

We can observe from Figure 4(b) that the adaptive approach presents a remarkable agreement with the filtered DNS data. In contrast, the standard DG-VMS approach and the ILES appear to overestimate the total amount of enstrophy beyond $t \approx 6$, suggesting an insufficient amount of dissipation in these simulations. Furthermore, the ILES exhibits multiple (unphysical) peaks, which might be caused by aliasing effects. It is also visible from Figure 4(a) that the adaptive DG-VMS achieves an improved level of accuracy of $\mathcal{K}$ predictions as compared to its non-adaptive counterpart and the ILES, with an evolution of $\mathcal{K}$ that practically falls on top of the reference. The low levels of $\mathcal{K}$ displayed by the standard DG-VMS in the final stages of the simulation can be explained by the fact that for this value of p_L the method is not able to provide sufficient dissipation during the transition phase leading to a proliferation of small scales and consequently to an overdissipative behavior past the peak of enstrophy ($t > 9$). This unsatisfactory behavior is avoided in the adaptive DG-VMS algorithm by progressively reducing the local scale-partition parameter during the transition phase and slowly increasing it during the dissipation phase, as shown in Figure 5.

To analyze the sensitivity of the adaptive approach to the parameters σ_{th} and β, the evolutions of the enstrophy obtained for several values of these parameters are shown in Figure 6. As expected, higher values of β and σ_K lead to lower levels of enstrophy caused by a higher amount of dissipation in the simulations. However, only limited differences can be observed, which leads to the conclusion that the sensitivity of the solution to the values of these two parameters is low, notably if compared to the sensitivity of the standard DG-VMS to the scale-partition parameter (Figure 7). These results suggest

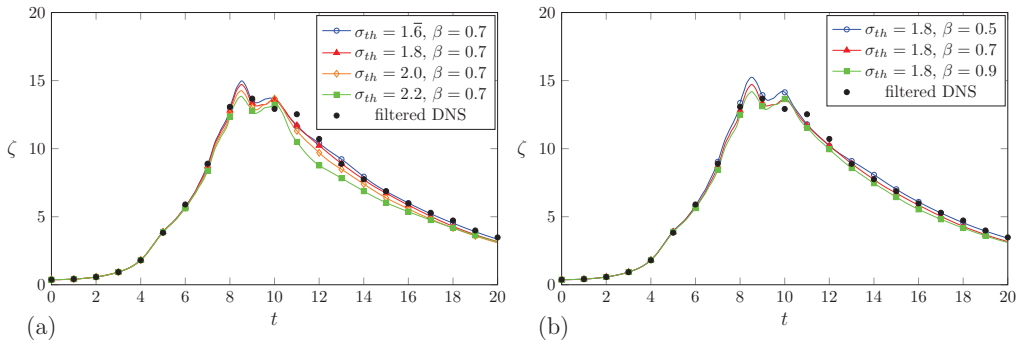

FIGURE 6. TGV at $Re = 5,000$: sensitivity of the evolution of the resolved enstrophy for the adaptive VMS approach to the model parameters: σ_{th} (left) and β (right).

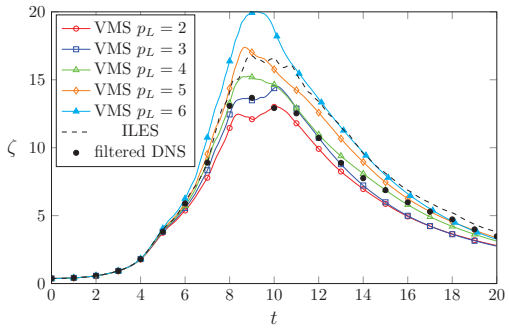

FIGURE 7. TGV at $Re = 5,000$: sensitivity of the evolution of the resolved enstrophy for the standard VMS approach to the scale-partition parameter p_L.

that the adaptive DG-VMS model proposed here can significantly improve the results and provide a more robust approach as compared to its standard counterpart.

4. Conclusions

This work analyzes the spectral properties of the DG-VMS approach to LES by performing *a-priori* tests of the inter-scale energy transfer in Fourier space. A consistent methodology has been proposed to evaluate the ideal SGS stresses from DNS data including the effect of the DG filter. The DG filter introduces discontinuities in the filtered field that need to be taken into account to properly evaluate the ideal SGS stresses. The ideal energy transfer has therefore been evaluated from DNS data of the TGV at $Re = 5,000$ and $Re = 20,000$ for various *hp*-discretizations and compared to the energy transfer provided by the DG-VMS approach based on the Smagorinsky model. For both Reynolds numbers at sufficiently fine resolutions, the energy transfer between large and unresolved scales can be neglected. It has also been demonstrated that the DG-VMS approach can accurately approximate the ideal energy transfer when appropriate values of the scale-partition parameter p_L and the model constant are selected. The values of these two parameters will necessarily depend on the level of resolution of the problem at hand. The decay rate of the modal energy also exhibits a correlation with the ideal value of p_L.

Based on these results, we have developed a locally adaptive DG-VMS strategy allowing

us to adjust the VMS partition in space and time. It relies on the estimation of the decay rate of the modal energy spectrum as an indicator of the local smoothness of the solution. The adaptive DG-VMS approach has provided promising results for the LES of the TGV at $Re = 5,000$ considering a very coarse mesh ($1/14^3$ of the DNS resolution). The adaptive algorithm actually yields improved accuracy and robustness as compared to its standard counterpart. More extensive analyses need to be carried out to evaluate the generality of the proposed algorithm for different *hp*-discretizations and more complex configurations.

Acknowledgments

This work was performed using HPC resources from CINES and TGCC (GENCI Grant 2017-A0022A10129 and 2017-A0032A07624).

REFERENCES

Chapelier, J.-B., de la Llave Plata, M. & Lamballais, E. 2016 Development of a multiscale LES model in the context of a modal discontinuous Galerkin method. *Comput. Method Appl. M* **307**, 275–299.

Chapelier, J.-B. & Lodato, G. 2016 A spectral-element dynamic model for the large-eddy simulation of turbulent flows. *J. Comput. Phys.* **321**, 279–302.

Cockburn, B. & Shu, C.-W. 2001 Runge–Kutta discontinuous Galerkin methods for convection-dominated problems. *J. Sci. Comput.* **16** (3), 173–261.

Dairay, T., Lamballais, E., Laizet, S. & Vassilicos, J. C. 2017 Numerical dissipation vs. subgrid-scale modelling for LES. *J. Comput. Phys.* **337**, 252–274.

Gottlieb, D. & Orszag, S. A. 1977 *Numerical Analysis of Spectral Methods: Theory and Applications*, vol. 26, SIAM.

Hughes, T. J. R., Mazzei, L. & Jansen, K. E. 2000 Large eddy simulation and the variational multiscale method. *Comput. Visual. Sci.* **3**, 47–59.

Hughes, T. J. R., Wells, G. N. & Wray, A. A. 2004 Energy transfers and spectral eddy viscosity in large-eddy simulations of homogeneous isotropic turbulence: Comparison of dynamic Smagorinsky and multiscale models over a range of discretizations. *Phys. Fluids* **16**, 4044–4052.

Lamballais, E., Dairay, T., Laizet, S. & Vassilicos, J. C. 2017 Implicit/explicit spectral viscosity and large-scale SGS effects. In *ERCOFTAC Workshop Direct and Large-Eddy Simulation 11, DLES11*.

Lamballais, E., Métais, O. & Lesieur, M. 1998 Spectral-dynamic model for large-eddy simulations of turbulent rotating channel flow. *Theoret. Comput. Fluid Dyn.* **12**, 149–177.

Pope, S. 2001 Large-eddy simulation using projection onto local basis functions. In *Fluid Mechanics and the Environment: Dynamical Approaches*, pp. 239–265. Springer.

Sagaut, P. & Levasseur, V. 2005 Sensitivity of spectral variational multiscale methods for large-eddy simulation of isotropic turbulence. *Phys. Fluids* **17**, 035113.

Vreman, A. 2004 The adjoint filter operator in large-eddy simulation of turbulent flow. *Phys. Fluids* **16**, 2012–2022.